Journal of Cleaner Production 84 (2014) 589–596

Contents lists available at ScienceDirect

Journal of Cleaner Production

journal homepage: www.elsevier.com/locate/jclepro

Note from the field

Identifying the relative importance of energy and water costs in hydraulic transport systems through a combined physics- and cost-based indicator

Christian F. Ihle [a,b,*], Aldo Tamburrino [c,b], Santiago Montserrat [b]

[a] Department of Mining Engineering, Universidad de Chile, Av. Tupper 2069, 8370451 Santiago, Chile[1]
[b] Advanced Mining Technology Center, Universidad de Chile, Blanco Encalada 2002, Santiago, Chile[2]
[c] Department of Civil Engineering, Universidad de Chile, Blanco Encalada 2002, Santiago, Chile[2]

ARTICLE INFO

Article history:
Received 31 May 2013
Received in revised form
12 November 2013
Accepted 20 November 2013
Available online 5 December 2013

Keywords:
Ore concentrate
Energy efficiency
Slurry pipelines
Long distance pipelines
Dimensionless number
Sustainability

ABSTRACT

Modern long distance ore pipeline systems are subject to strong costs, both from the economic and environmental standpoints. The task of assessing the relative importance of energy and water consumption without a detailed engineering analysis is often not obvious. In the present paper, the relative importance of water and energy unit costs is assessed by a novel dimensionless formulation accounting for the essential hydraulic and cost elements that conform the slurry transport. It is found that, for conditions resembling those of copper and iron concentrate pipelines, the ratio between energy and water costs has a wide range, depending on the particular transport conditions and unit cost scenarios. Although operating at similar volume fractions, results indicate that energy/water cost relations may differ between copper and iron concentrate pipelines and local conditions, thus suggesting the need to explicitly include energy and water cost in the design strategy.

1. Introduction

The new challenges that modern slurry engineering faces include the need not only to take into account environmental variables such as carbon footprint at project and operation phases (Norgate and Haque, 2010; Ihle, 2014), but also to apply design criteria according to the local economical, environmental and resource reality. In particular, water scarcity adds an additional variable to the complex problem of project infrastructure and/or subsequent operation decision: should an optimal combination of design and/or operational parameters be influenced by water and energy costs? The answer seems to be affirmative, not only due to the economic implications it has, but also due to the effect of location and community responses, which may have a strong local influence (see, e.g., Murguía and Böhling, 2013; for the case of Minera Alumbrera, Argentina, which features a 300 km-long copper concentrate pipeline). The presence of stakeholders (Jenkins, 2004; Jenkins and Yakovleva, 2006; Newbold, 2006) in the form of geography, demography, alternative resource users, the regulatory framework (Oyarzún and Oyarzún, 2011) and the idiosyncrasy of communities located in different regions of different countries might then, *ceteris paribus*, suggest different infrastructure solutions.

Despite the need, as in any other industrial process, to minimize both water and energy consumption in the mining sector, the hydraulic transport of ore concentrates faces a new dilemma. At equal dry tonnages, reducing the amount of water causes an increase on the slurry concentration, with a subsequent increase of the energy requirement, and potential water/energy consumption scenarios may be seen as the result of the competition energy and water costs (Ihle, 2013). The task of putting together the costs of water and energy needs to be completed with some means of hydraulic expected behavior. At this point, it is the system hydraulics —whose key elements are referred herein— that which gives completeness to a water vs. energy cost balance, thus departing from a more simplistic but incomplete unit cost ratio approach. Such a (non-dimensional) ratio is given in Section 2.1. The pursued outcome is to be able to give an *ex-ante* assessment of the relative impact of water and energy in a prospective system. The main intent is to seek for engineering strategies or design approaches that might be biased

* Corresponding author. Department of Mining Engineering, Universidad de Chile, Av. Tupper 2069, 8370451 Santiago, Chile. Tel.: +56 2 29784503.
E-mail address: cihle@ing.uchile.cl (C.F. Ihle).
[1] Tel.: +56 2 29784503.
[2] Tel.: +56 2 29784400.

0959-6526/$ – see front matter © 2013 Elsevier Ltd. All rights reserved.
http://dx.doi.org/10.1016/j.jclepro.2013.11.070

towards greater energy or water savings depending on variables like the required system capacity, system length and diameter, and slurry properties. The present approach is therefore seen as a first step in an environmental management (Hilson and Nayee, 2002) and a cleaner production framework (Hilson, 2003) through the effective integration of process, environmental and social aspects.

In slurry transport, water acts as a mere vehicle for the granular matter containing the mineral; is required in considerable quantities and is obtained from diverse sources, including aquifers and the sea. Disregarding additional social or environmental components, the cost of water, depending on whether it comes from aquifer or a desalinated plant, may fluctuate depending on their origin and potential pre-treatment requirements (Ihle, 2013). On the other hand, energy costs may significantly vary according to local and global aspects. In particular, the Chilean energy costs are different than those in Brazil, Perú and Argentina (Del Campo, 2012).

Pumping ore slurries through long distances, which commonly exceed 100 km, requires electrical powers that may exceed several megawatts during steady operation. The inherently nonlinear nature of transport often makes an *a priori* assessment of the relative importance of water and energy a non trivial task. Assuming that water and energy unit costs (c_W and c_E) have units of currency over energy and currency over water volume, respectively, the resulting ratio has units of volume over energy, which is conditioned by factors such as the slurry mean flow, solids volume fraction, diameter and length. In this paper, a set of order of magnitude relations grasping the essential features of the hydraulic behavior of long distance ore transport systems are obtained from the literature and cast into a dimensionless number accounting for the relative effect of water and energy costs, with regard to the specific case of iron and copper concentrates.

2. Dimensionless number formulation

2.1. General form of the dimensionless number Π

Consider the water and energy required to transport a given amount of dry concentrate per unit time, $\dot{m}$, over a distance L. The total combined cost of water and energy may be simply expressed as:

$$\Omega = c_E E + c_W W, \tag{1}$$

where c_E, c_W, E and W are the energy and water unit costs, the total energy and water spent, respectively. Ω is therefore expressed as currency units per period, whereas E and W are given as energy and water volume spent per period. Unit costs need to be consistent with those of energy and water costs. The energy consumption, E, is computed from the pipeline characteristics and route, including the topography. In particular, an energy balance between points 1 and 2 of a turbulent flow stream across the pipeline is given by:

$$\frac{p_1}{\rho_m g} + z_1 = \frac{p_2}{\rho_m g} + z_2 + \mathrm{J}L_{12}, \tag{2}$$

with $J = f/DU^2/2g$ the hydraulic gradient. Here p_i and z_i=$z(x$=$x_i)$ are the line pressure and altitude at the route point x_i, assuming the flow going from point x_1 to x_2, distant by a tube length L_{12}, and g is the magnitude of the gravity acceleration vector. The last term of the right hand side of (2) represent the frictional pressure losses, which control the energy balance. There, the Darcy friction factor, f, is defined as $f = 8\tau_w/\rho_m U^2$, with τ_w, ρ_m and U the wall shear stress, slurry density and mean flow velocity, respectively, and D the pipeline internal diameter. Assuming that the pump station delivers the slurry at a pressure p_1, that the pipeline has a constant internal diameter and that the corresponding pressure is consistent with restrictions including the pipeline pressure rating and possibly the need to operate above the vapor pressure at all times, the required pumping power may be expressed in terms of the flow rate (Q) as $p_1 Q/\varepsilon_p$, with ε_p the pumping efficiency. Provided an operation at constant flow rate, it may be integrated over a period λT (λ<1), to obtain the total energy consumption over a period T, with a system utilization λ, as $E = p_1 Q/\varepsilon_p \lambda T$, where the flow rate ($Q$) is possibly a function of the solids volume fraction, ϕ. This implies that the pipeline is idle a total amount of $(1-\lambda)T$ seconds per period, where the rest of the time it delivers concentrate at mean flow rate, with a total amount of dry solids delivered equal to $\dot{m}T$. Here, for the sake of a clear analytical interpretation of the various terms including the energy balance and water consumption, the simple geometry of a constant internal diameter horizontal tube will be considered. However, the inclusion of local topographic effects or multiple diameters is straightforward from the energy balance perspective, as described. The corresponding energy requirement is expressed as (Ihle, 2013):

$$E = \frac{\lambda T \rho_m Q}{\varepsilon_p}\left[\frac{p(x = L)}{\rho_m} + \frac{8fLQ^2}{D^5\pi^2}\right], \tag{3}$$

where L is the overall pipeline length. The first term in the brackets is the pressure near the delivery point (x=L), which may be that of atmosphere or a higher value if dissipation, characterized by an energy dissipation coefficient, K, is imposed to avoid slack flow ($p \gtrsim 0$) due to topography: $p(x$=$L) \approx 8\rho_m K Q^2/\pi^2 D^2$. When energy generation is chosen instead of energy dissipation, K becomes a characteristic of the hydraulic power amenable to be obtained by the corresponding turbine. The present analysis will be rather centered in the effects of friction, which commonly dominate in long distance slurry pipelines, and therefore K=0—i.e. $p(x$=$L)$= 0— is assumed herein.

The amount of consumed water may be obtained by virtue of mass conservation (Ihle and Tamburrino, 2012c; Ihle, 2013):

$$\dot{m} = \lambda Q \phi S \rho_W \tag{4a}$$

$$W = \frac{\dot{m}T}{S\rho_W}\left(\frac{1}{\phi} - 1\right), \tag{4b}$$

where $\dot{m}$ is the dry solids transport rate (also referred to as throughput), S is the specific gravity of solids and ρ_W is the density of the carrier fluid, typically clear process water.

Using (3) and (4), a general relation in terms of the friction factor, with the aforementioned set of hypotheses, is expressed as:

$$\Pi_0 = \frac{c_E E}{c_W W} = \frac{8f\rho_m Q^2 L c_E}{\varepsilon_p D^5 \pi^2 (1-\phi) c_W}. \tag{5}$$

This dimensionless number is fairly general and requires, in particular, the knowledge of the flow rate, Q, which is strongly dependent on the throughput ($\dot{m}$), the pipeline diameter and a way to characterize the Darcy friction factor f. Unless a preliminary pipeline calculation has been done, an estimation of Π_0 in prospective systems is not straightforward. However, it is possible to parameterize it for a more intuitive applicability by imposing two key conditions for the flow. First, it is often required that transport needs to be in turbulent flow, with the mean flow velocity above the laminar-turbulent transition. On the other hand, particles are required to be kept in suspension, and therefore, the flow velocity must exceed the deposit limit.

2.2. Minimum velocity characterization

2.2.1. Rheology

It is instructive to parameterize it in terms of a particular slurry rheology and a frictional law. It is assumed that the slurry is well-described using the Bingham model (Chhabra and Richardson, 2008):

$$\eta\frac{\partial u}{\partial z} = \begin{cases} 0 & \text{if } |\tau| < \tau_y \\ \tau - \tau_y \mathrm{sgn}\left(\frac{\partial u}{\partial z}\right) & \text{if } |\tau| \geq \tau_y, \end{cases} \tag{6}$$

where u, η, τ and τ_y are the component of velocity along the pipe axis, Bingham (dynamic) plastic viscosity, shear and yield stress, respectively. The function sgn is defined as $\mathrm{sgn}(x)=x/|x|$ if $x\neq 0$ and 0 otherwise. Both the plastic viscosity and yield stress depend on the solids volume concentration ϕ. The former is commonly expressed by the simple relation (Barnes, 2000):

$$\frac{\eta}{\mu} = \left(1-\frac{\phi}{\phi_{ss}}\right)^{-\beta_\eta}, \tag{7}$$

where μ is the liquid viscosity, β_η is a constant and φ_{ss} is the loose packing concentration. In particular, $(\beta_\eta,\varphi_{ss})=(2,0.47)$ give a reasonable approximation of the viscosity of many copper and iron ore concentrates at concentrations not very close to φ_{ss} (Ihle, 2013). The identification of the yield stress has a related origin, and thus is often expressed similarly as (Heymann et al., 2002; Barnes, 2000):

$$\tau_y = \frac{\widehat{\tau}}{(\phi-\phi_{ss})^{\beta_y}}, \tag{8}$$

where $\widehat{\tau}$ and β_y are empirical parameters, with the former having dimensions of shear stress and the latter being dimensionless. For the purposes of obtaining numerical values on the order of those of copper and iron concentrates, the empirical parameters $(\beta_y,\widehat{\tau}) = (2, 0.038)$, similar to those used in Ihle and Tamburrino (2012c), will be considered herein.

2.2.2. Laminar-turbulent transition

The small, albeit non-negligible yield stress (typically below 1 Pa in iron and copper concentrate slurries at common transport concentrations) is mostly relevant to characterize the laminar-turbulent transition, *via* the Bingham and Reynolds numbers, $B=\tau_y D/U\eta$ and $Re=\rho_m UD/\eta$, representing the ratios of yield to viscous stresses and inertial to viscous forces, respectively. For various values of the Bingham number, the laminar-turbulent transition may be characterized as different power laws for B (Nouar and Frigaard, 2001). Equivalently, in terms of the Hestrom number, $He=ReB=\rho_m\tau_y D^2/\eta^2$, the laminar-turbulent transition may be scaled as

$$Re_c \approx \alpha_t He^{\beta_t}, \tag{9}$$

where for Hedström numbers exceeding 1.5×10^5, corresponding to typical copper and iron ore concentrate transport lines (with larger values in the latter case), the empirical fit $\alpha_t \approx 26$ and $\beta_t = 1/2$ (Slatter and Wasp, 2000). The corresponding transition velocity, defined as U_t, is given by $U_t=Re_c\eta/\rho_m D$.

2.2.3. Deposition velocity

A condition for the critical depositional velocity, U_d, may be expressed using scaling arguments as a functional relation between a Froude number, $\mathrm{Fr} = U_d/\sqrt{gD(S-1)}$, representing a balance between inertial forces and gravity, and an Archimedes number, standing for a balance between particle buoyancy and viscous forces —$\mathrm{Ar} = 4/3gd_{50}(S-1)\rho_m/\eta^2$, with d_{50} the median particle diameter and g the acceleration of gravity—, as $\mathrm{Fr}\approx\alpha_d\mathrm{Ar}^{\beta_d}$ (Shook et al., 2002) or, equivalently,

$$U_d = \alpha_d[gD(S-1)]^{1/2}\mathrm{Ar}^{\beta_d}. \tag{10}$$

For the particle size range of copper and iron concentrates, the depositional velocity has been successfully correlated by Poloski et al. (2010) using (10) with $\alpha_d = 0.59$ and $\beta_d = 0.15$.

The minimum transport velocity may be estimated as that which exceeds both the laminar-turbulent transitional threshold and depositional value. Considering the design factors k_t and k_d for each of them, respectively, a measure of the minimum velocity may be therefore expressed as $U_{\min} = \max[k_tU_t,k_dU_d]$.

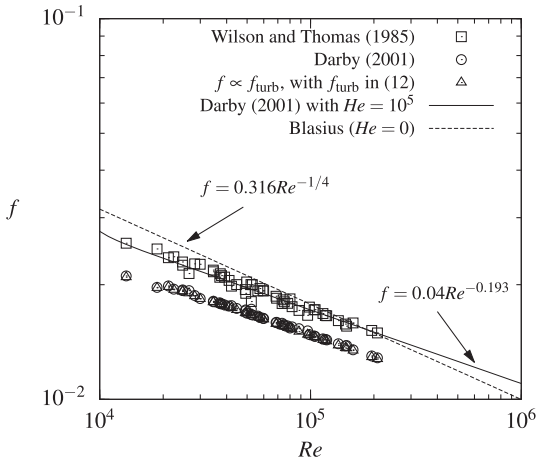

Fig. 1. Comparison between power law models for Darcy friction factor calculations (f) and the Wilson-Thomas model, based on the logarithmic velocity profile (Wilson and Thomas, 1985), in terms of the Reynolds number, $\mathrm{Re} = \rho_m\mathrm{UD}/\eta$. The symbols represent several calculation instances, with Hedström numbers, $\mathrm{He} = \rho_m\tau_y D^2/\eta^2$, ranging from 10^5 to 4.5×10^6, whereas the lines stand for constant Hedström numbers, indicated in the legend.

2.3. Friction factor

To obtain order of magnitude figures for the case of copper and iron concentrate flows, whose most typical dynamical regime is that of smooth wall friction, the friction factor may be expressed as a strong function of the Reynolds number and perhaps a weak function of the non-Newtonian characteristic of the slurry. In most copper and iron concentrates, the yield stress is small compared to the wall shear stress and thus, at moderate Reynolds numbers and flow rates above the minimum value, the slurry effectively flows similarly as a Newtonian one with little effect of the stratification due to the presence of solids, as discussed elsewhere (Ihle and Tamburrino, 2012b). It is thus a valid approximation for many applications to assume that the friction factor is given by a simple power law:

$$f \approx \alpha_f \mathrm{Re}^{-\beta_f}. \tag{11}$$

For turbulent flow of Bingham fluids with $\mathrm{Re}\gtrsim10^4$, Darby (2001) proposed a combination of a laminar (f_{lam}) and a turbulent (f_{turb}) friction factor through the metric

$$f = 4\left(f_{\mathrm{lam}}^{1/e} + f_{\mathrm{turb}}^{1/e}\right)^e, \tag{12}$$

with e an empirical parameter, f_{lam} obtained from the solution of the Buckingham equation (Ihle and Tamburrino, 2012a) and f_{turb}

proportional to $Re^{-0.193}$. Such exponent clearly resembles the value of 0.25 of the Blasius power law for smooth turbulence regime. Similarly, Chilton and Stainsby (1998) proposed a modification of the Reynolds number, directly keeping the parameters in the Blasius relation: $f = 4 \cdot 0.079 \cdot (1-\tau_y/\tau_w) Re^{-0.25}$. For a mean flow velocity of 1.5 m/s and a yield stress close to 0.3 Pa, the wall shear stress τ_w is on the order of 10 Pa, and $\tau_y/\tau_w \approx 0.03$. Fig. 1 shows some results of friction factors obtained for yield stresses between 0.6 Pa and 1.8 Pa and Reynolds numbers between 10^4 and 2×10^5, representing the typical range for copper and iron concentrates. Power law correlations are compared with the Wilson-Thomas model (Wilson and Thomas, 1985; Thomas and Wilson, 1987), consisting of an extension of the logarithmic velocity profile to yield pseudoplastic fluids. For the purposes of the present order of magnitude analysis, the Darcy friction may be therefore estimated using a power law as in (11), as shown in Fig. 1. Here, the Blasius power law $(\alpha_f,\beta_f)=(0.316,0.25)$ will be considered.

To have a rough estimation of the relative importance of the energy and water costs, the dimensionless relation (5) may be evaluated without a detailed knowledge of the system hydraulic behavior, by means of (7), (8), (9) and (10), with proper assumptions of the model parameter coefficients β_η, β_y, α_t, β_t, α_d, β_d, α_f, β_f, k_d and k_t.

2.4. Critical concentration for the minimum velocity form

The relations presented in the previous section are strongly dependent on the solids concentration, ϕ, and the specific gravity of solids, S. Although the dimensionless number Π_0 has a relatively general use, its dependence on such variables is not evident. However, given the slurry and pipeline properties, the minimum velocity, $U_{\min}$, is controlled by the deposit velocity and the laminar-turbulent transition for concentrations below and above a critical value (Ihle and Tamburrino, 2012b), where the former is a monotonically decreasing function of concentration and the latter a monotonically increasing one. Equating $k_t U_t$, with U_t from (9) (laminar-turbulent transition) and $k_d U_d$, with U_d from (10) (solids deposition mechanism), and noting that $\rho_m/\rho_W = S\varphi + 1 - \varphi$, an equation for the concentration φ_*, corresponding to the absolute minimum of the $U_{\min}(\varphi)$ envelope, is found:

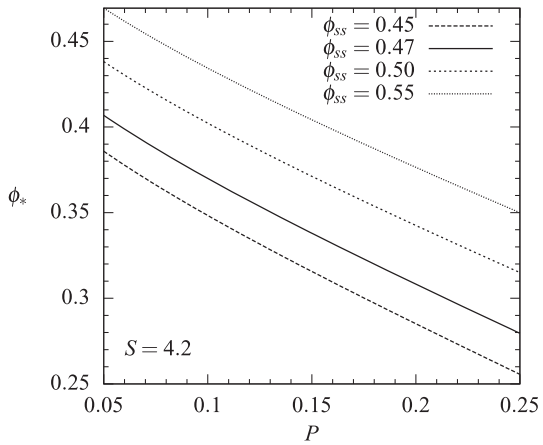

Fig. 2. Critical value of the solids volume concentration, φ_*, for which the deposit velocity (augmented by a factor $k_d = 2$) equals the laminar-turbulent transition velocity (Eq. (13)), multiplied by $k_t = 2$, for $S = 4.2$ φ_{ss}, in terms of the dimensionless number P (15). The model parameters are defined as $\beta_\eta = 2$, $\beta_y = 2$, $\alpha_t = 26$, $\beta_t = 1/2$, $\alpha_d = 0.59$, and $\beta_d = 0.15$.

$$(S\phi_* + 1 - \phi_*)^{a_{1*}} (S-1)^{a_{2*}} - P(\phi_{ss} - \phi_*)^{a_{3*}} = 0, \tag{13}$$

with:

$$a_{1*} = 1 + 2\beta_d - \beta_t \tag{14a}$$

$$a_{2*} = \beta_d + \frac{1}{2} \tag{14b}$$

$$a_{3*} = \beta_\eta [2(\beta_t - \beta_d) - 1] - \beta_y \beta_t, \tag{14c}$$

and the dimensionless number P defined as:

$$P = \frac{1}{A^{\beta_d}} \frac{k_t \alpha_t}{k_d \alpha_d} \left(\frac{\widehat{\tau} \rho_W D^2}{\mu^2} \right)^{\beta_\eta} \left(\frac{\mu}{\rho_W g^{1/2} D^{3/2}} \right) \frac{1}{\phi_{ss}^{\beta_\eta [2(\beta_t - \beta_d) - 1]}}. \tag{15}$$

Here, $A = 4/3 g d_{50}^3 (\rho_W/\mu)^2$, obtained from rewriting the Archimedes number introduced in (10). Fig. 2 shows a set of solutions for typical parameter values.

2.5. Simplified expressions for Π_0

The value obtained in (13) defines two alternative ways to write the dimensionless number (5), depending whether it is the deposit velocity or the laminar-turbulent transition velocity that which needs to be considered. In either case, the new dimensionless number Π has the general form:

$$\Pi \approx \gamma \Psi(\phi, S) \Lambda^{\beta_f} \Gamma, \tag{16}$$

where the form of the dimensionless function $\gamma\Psi$ and the dimensionless numbers Λ and Γ depend on whether ϕ is greater than φ_*. When $\varphi < \varphi_*$ the minimum velocity is controlled by the deposit velocity criterion (10), whence the dimensionless constant $\gamma = \gamma_d$, $\Psi = \Psi_d$, $\Lambda = \Lambda_d$ and $\Gamma = \Gamma_d$ with:

$$\gamma_d = \gamma_0 (k_d \alpha_d)^{2-\beta_f} \tag{17a}$$

$$\Psi_d(\phi, S) = \frac{(S\phi + 1 - \phi)^{a_{1d}}}{1 - \phi} \left(\frac{\phi_{ss}}{\phi_{ss} - \phi} \right)^{a_{2d}} (S-1)^{a_{3d}} \tag{17b}$$

$$\Lambda_d = \frac{1}{A^{\beta_d}} \frac{\mu}{\rho_W g^{1/2} D^{3/2}} \tag{17c}$$

$$\Gamma_d = A^{2\beta_d} g \rho_W \frac{c_E}{c_W} L \tag{17d}$$

with the exponents a_{1d}, a_{2d} and a_{3d} defined as:

$$a_{1d} = 1 - \beta_f + 2\beta_d \left(2 - \beta_f\right) \tag{18a}$$

$$a_{2d} = \beta_\eta \left[\beta_f - 2\beta_d \left(2 - \beta_f\right) \right] \tag{18b}$$

$$a_{3d} = \left(2 - \beta_f\right) \left(\beta_d + \frac{1}{2}\right) \tag{18c}$$

and

$$\gamma_0 = \frac{\alpha_f}{2\varepsilon_p} \tag{19}$$

On the other hand, when the minimum velocity is controlled by the laminar-turbulent transition ($\varphi \geq \varphi^*$), the components of (16) take the form:

$$\gamma_t = \gamma_0 (k_t \alpha_t)^{2-\beta_f} \tag{20a}$$

$$\Psi_t(\phi, S) = \frac{(S\phi + 1 - \phi)^{a_{1t}} \phi_{ss}^{a_{2t}}}{(1-\phi)(\phi_{ss} - \phi)^{a_{3t}}} \tag{20b}$$

$$\Lambda_t = \left(\frac{\mu^2}{\rho_W^2 D^2 \widehat{\tau}} \right)^{\beta_t} \tag{20c}$$

$$\Gamma_t = \left(\frac{\rho_W D^2 \widehat{\tau}}{\mu^2} \right)^{2\beta_t} \frac{\mu^2 L}{\rho_W D^3} \frac{c_E}{c_W}, \tag{20d}$$

with γ_0 given by (19) and

$$a_{1t} = \beta_t \left(2 - \beta_f\right) - 1 \tag{21a}$$

$$a_{2t} = 2\left[1 - \beta_t \left(2 - \beta_f\right)\right] \tag{21b}$$

$$a_{3t} = \beta_y \beta_t \left(2 - \beta_f\right). \tag{21c}$$

In summary, the dimensionless number Π, given by (16) may be roughly estimated following the steps as below:

1. Identify proper values of D, L, S, ϕ, c_E, c_W, d_{50}, $\widehat{\tau}$, φ_{ss}, and the dimensionless model parameters β_η, β_y, α_t, β_t, α_d, β_d, and ε_p.
2. Solve (13) for φ^* using (15), which may be evaluated with the aforementioned input data.
3. If $\varphi < \varphi^*$, then evaluate Π using (17), (18) and (19). If $\varphi \geq \varphi^*$, evaluate Π using (19), (20), and (21).

The dimensionless model parameters referred in the numeral 1 may be obtained either from the literature or from direct experimental measurements when possible. Although the combined effect of inaccuracies in their identification may be a significant source of uncertainty in the cost terms (Ihle et al., 2013), for very large *or* small values of Π, small uncertainties in them should not lead to misleading results. This is not, however, the case for order 1 values of Π, where errors on in the determination of input parameters might drive to erroneous conclusions.

3. Discussion

It is seen from the structure of (16), (17) and (20) that both Λ_d and Λ_t depend in the same way on the frictional law, β_f, but at either regime the dimensionless number Γ depends only on the form of the applicable minimum velocity criterion but not on the pressure loss model parameters. While in Γ_d there is no diameter term, i.e., the effect of particle deposition is only apparent when coupled to the pressure loss model, in Γ_t there is a part of such number which is independent of β_f but dependent on the laminar-turbulent transition parameter, β_t. Choosing a reference number $\beta_t = 1/2$, Γ_t becomes inversely proportional to the diameter.

Fig. 3 shows the structure of Ψ_d and Ψ_t for the same parameters used in the example depicted in Fig. 2. In Ψ_d, where the deposit velocity condition dominates, a local maximum is observed. This is explained by the relative importance of the specific gravity of the slurry, $\rho_m/\rho_W = S\varphi + 1 - \varphi$, and the slurry relative viscosity, $\eta/\mu = (\phi_{ss}/\phi_{ss} - \phi)^{\beta_\eta}$, where the growth rate of the former, $\delta\rho_m/$

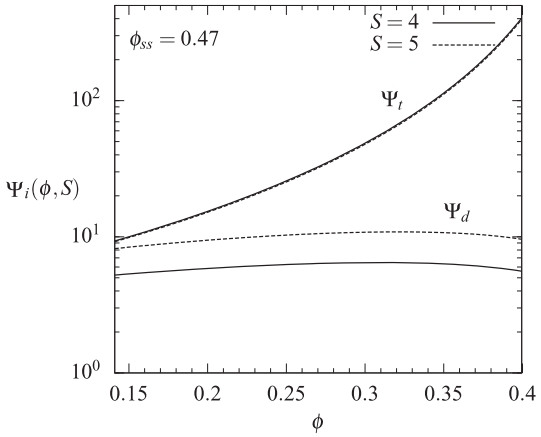

Fig. 3. The functions Ψ_d (17b) and Ψ_t (20b) in terms of the solids volume fraction, ϕ, assuming $\beta_\eta = 2$, $\beta_y = 2$, $\alpha_t = 26$, $\beta_t = 1/2$, $\alpha_d = 0.59$, and $\beta_d = 0.15$.

$\rho_m = S - 1/\varphi(S-1) + 1$ is positive but decreases with concentration to a minimum value equal to $S - 1/\varphi_{ss}(S-1) + 1$. In contrast, the negative growth rate of the relative viscosity in terms of the concentration, $\delta\eta/\eta = -1/(\phi_{ss} - \phi)^{\beta_\eta}$, is small for small concentrations but becomes asymptotically large when ϕ approaches φ_{ss}. Differently, the function Ψ_t, which applies when the laminar-turbulent transition controls the minimum velocity, is strongly controlled by the concentration through the viscosity, as $U_t \sim (S\phi + 1 - \phi)^{(\beta_t - 1)} / (\phi_{ss} - \phi)^{\beta_y \beta_t + (1 - 2\beta_t)\beta_\eta} \approx 1/(S\phi + 1 - \phi)^{1/2} (\phi_{ss} - \phi)$, the last relation applying using typical parameters for the transition velocity, yield stress and viscosity. For concentrations approaching φ_{ss}, Ψ_t grows unboundedly. On the other hand, S, causing a decrease on Ψ_t, have slight effect on the resulting function. The structure of the functions Ψ_d and Ψ_t has two key implications: for $\varphi < \varphi^*$, Ψ has a moderate dependence on the specific gravity of solids and is relatively insensitive to concentration, whereas for $\varphi > \varphi^*$ it is the volume fraction that which mostly controls Ψ.

The overall effect of concentration and energy-water unit costs on the energy-water cost ratio Π may be exemplified for conditions typical to copper and iron concentrates. Fig. 4 shows the effect of

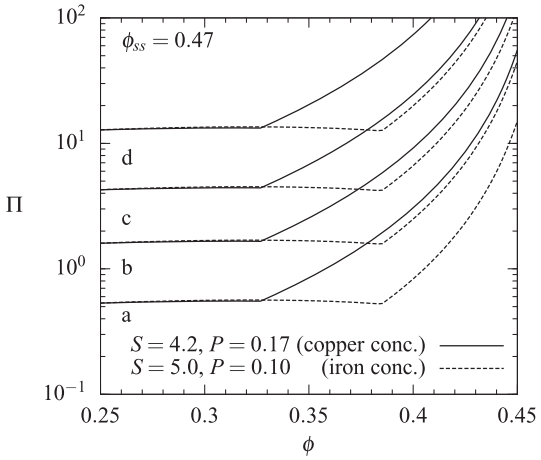

Fig. 4. Dependence of the dimensionless number Π on the concentration (ϕ) for conditions resembling a $L = 200$ km copper concentrate line ($S = 4.2$, computed using a 6-inch nominal diameter) and an iron concentrate pipeline ($S = 5$, computed using a 18-inch nominal diameter) of the same length, with $\varphi_{ss} = 0.47$. (a) $c_E = 50$ USD/MWh and $c_W = 4$ USD/m^3; (b) $c_E = 150$ USD/MWh and $c_W = 4$ USD/m^3; (c) $c_E = 50$ USD/MWh and $c_W = 0.5$ USD/m^3 and (d) $c_E = 150$ USD/MWh and $c_W = 0.5$ USD/m^3. The model parameters are defined as $\beta_\eta = 2$, $\beta_y = 2$, $\alpha_t = 26$, $\beta_t = 1/2$, $\alpha_d = 0.59$, $\beta_d = 0.15$, $\varepsilon_p = 0.7$, and $k_t = k_d = 2$.

four different combinations of c_E and c_W. The present model shows that for the copper concentrate line and volume fractions close to 0.35, Π is mostly controlled by the laminar-turbulent transition value, corresponding to that at the right of the abrupt change on the curve. Differently, around the same concentration the values of Π for iron concentrate are rather controlled by the deposit velocity values.

Fig. 4 suggests that the effect of the different combinations of energy and water unit costs might cause widely different trends regarding whether it is water (set of curves (a), low to moderate concentrations) or energy (set of curves (d)) that which controls the cost relation Π. A sort of intermediate situation is found when both components are similarly important, depending on the concentration and the value of S, as depicted in curves (a) and (b). Even narrowing the concentration range to represent typical operational conditions, the result is similar. This is shown in Fig. 5, where both for copper and iron concentrate lines very low and high values of Π, corresponding to the prevalence of water and energy costs, respectively, were found.

The results shown in Fig. 5, although do not replace an in-depth optimization analysis to seek for best operational scenarios and/or infrastructure in terms of water and energy costs, give valuable insight to map cost drivers in different locations with distinct realities and operational requirements. Consider as an example the evaluation of two concentrate pipeline projects in two different location, say Chile (copper, with $S \approx 4.2$) and Brazil (iron, with $S \approx 5$). Even assuming similarities in transport characteristics (e.g $\varphi = 0.29$, a close-to-typical value for solids volume fraction and similar slurry parameters), tonnages —and thus diameters—, and total lengths differ. While Chilean concentrate pipelines commonly cross the country (i.e. span lengths between 100 and 200 km depending on the location) with nominal diameters between 6 and 9 inches, Brazilian ones may exceed 300 km with nominal diameters above 20 inches (see, e.g., the recent expansion of the 300 km Samarco pipeline and the 525 km long Minas Rio transport system; Jacobs, 1991; Betinol and Jaime, 2004; Silva et al., 2009; Correa et al., 2011). On the other hand, water and energy costs differ between both countries. While in Chile the mining sector faces the need to produce copper with high energy costs, a fact that partially affects the cost of water through the requirement of desalination and transportation from sea level to the Andes Mountains where the plants are commonly located, Brazil has lower water costs. Assuming the slurry properties —except the specific gravity of solids, pipeline lengths and diameters— and the model parameters used in Fig. 5, Table 1 shows the result of the application of the present methodology to assess the water/energy cost ratio as indicated earlier. Although present Chilean and Brazilian energy costs are not substantially different, Brazilian water is significantly less expensive. It is observed that the combined effect of larger tube lengths in iron ore lines and a more accessible water resource than in Chile makes comparatively more important the contribution of energy in light of the present results. In particular, the resulting value of Π in the Brazilian context appears to be on the order of 10, thus suggesting that it is energy rather than water consumption the main cost driver. On the other hand, in Chile, Π is rather close to 1, therefore implying that water and energy have a somewhat similar weight. Given the present data sources, this is not surprising when noting that an important part of the structure of the water cost is the cost of the energy required both for pumping and filtering —at least when the unit cost raise towards 4 USD/m^3—. An outcome of the present result is that optimal operational conditions in the Chilean example needs to be computed out of a formulation involving the cost of water, whereas in the Brazilian case if unit costs were well-defined —a thing that is not necessarily true— an energy efficiency approach disregarding water costs (Wu et al., 2010; Ihle and Tamburrino, 2012c) might give a good picture of the best choice of the flow rate, the solids concentration and the pipeline utilization ratio, given the plant throughput objective.

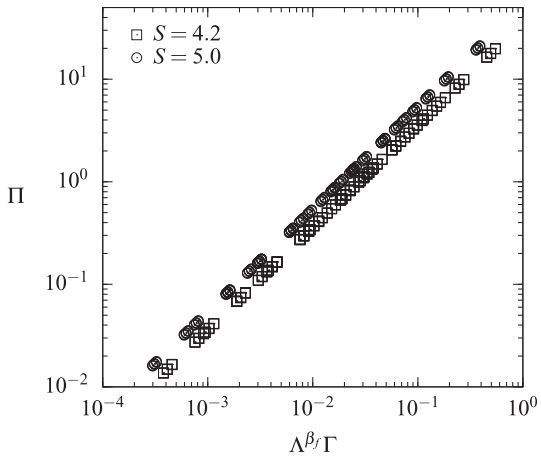

Fig. 5. Dependence of the dimensionless number Π on the dimensionless group $\Lambda^{\beta_f}\Gamma$, built upon various operational and geometric conditions. The squares represent a typical copper concentrate situation ($S = 4.2$), whereas the circles, an iron concentrate ($S = 5$), with $\varphi_{ss} = 0.47$. All possible combinations of the following input parameters have been considered: $\varphi = 0.28$, 0.3 and 0.32; $c_E = 30$, 75 and 150 USD/MWh; $c_W = 0.5$, 2 and 4 USD/m^3; $L = 10$, 100 and 300 km; $D_{\text{copper conc.}} = 6$, 8 and 10 inches (nominal), and $D_{\text{iron conc.}} = 16$, 18 and 20 inches (nominal). The model parameters are defined as $\beta_\eta = 2$, $\beta_y = 2$, $\alpha_t = 26$, $\beta_t = 1/2$, $\alpha_d = 0.59$, $\beta_d = 0.15$, $\varepsilon_p = 0.7$, and $k_t = k_d = 2$.

Table 1
Example of the effect of local conditions on values of the dimensionless parameter Π for conditions resembling typical Chilean (copper) and Brazilian (iron) concentrate pipelines. The ranges for the energy costs for Chile and Brazil are obtained from Sofofa (2013) and ANEEL (2013), respectively. Likewise, for water costs, Ihle (2013, and references therein) and Asad (1999) have been considered. The parameters φ_{ss}, β_t, α_d, β_d, ε_p, k_t and k_d are those referred in Fig. 5.

Case	Copper concentrate pipeline			Iron concentrate pipeline		
	$S = 4.2$, $D = 8$ in, $L = 100$ km			$S = 5$, $D = 20$ in, $L = 300$ km		
	c_E (USD/MWh)	c_W (USD/m^3)	Π –	c_E (USD/MWh)	c_W (USD/m^3)	Π –
1	110	1	2.4	80	0.5	10.3
2	150	1	3.3	120	0.5	15.4
3	110	2	1.2	80	0.75	6.9
4	150	2	1.7	120	0.75	10.3
5	110	4	0.6	80	1.0	5.1
6	150	4	0.8	120	1.0	7.7

The hypothetical situation depicted herein shows that hydraulic similarities do not necessarily imply that ore concentrate pipelines in different locations will have a similar impact regarding energy and water consumption. A key element that may limit the uptake of the present approach is, however, the ability to make a proper definition of the unit costs c_E and c_W. We have based our cost definitions solely on reference market values. A next challenge would be to find adequate values for an overall social water (McKinney, 1988) and energy cost (Viscusi et al., 1994; Söderholm and Sundqvist, 2003; Roth and Ambs, 2004), thus giving Π a broader significance.

Another implication of the present proposed dimensionless number is the potential to directly evaluate different water-energy relative cost scenarios through different possibilities involving the pipeline path —thus impacting the total tube length L—, as shown in (17d) and (20d).

4. Conclusions

It has been shown that the dimensionless number Π, representing the energy-water cost ratio, exposes the widely different conditions that different locations may imply. The form of the dimensionless number depends on whether the minimum transport velocity is conditioned by the solids deposition mechanism or by the laminar-turbulent transition. Regardless the particular choice of the expression for the dimensionless numbers Λ, Γ and $\Psi(\varphi,S)$, it has been identified that at typical transport concentrations the deposit mechanism tends to be stronger in iron concentrate lines whereas the laminar-turbulent transition is a stronger conditioner for Π in copper concentrate pipelines. Overall, Π may span several orders of magnitude, which somehow poses the validity of the challenge to integrate economics, environmental variables and system hydraulics for the next generation of long distance transport systems. An adequate use of the parameter is bonded to the need of a reasonable identification of water and energy costs. Critical to this purpose is to assess the impact of extra-economical variables which if were not considered, would yield to misleading conclusions.

Acknowledgments

The authors gratefully acknowledge support from the Departments of Civil Engineering and Mining Engineering of University of Chile, the Advanced Mining Technology Center of University of Chile and the Chilean National Commission for Scientific and Technological Research, CONICYT, through Fondecyt Project No. 11110201.

List of symbols

a	constant
A	dimensionless number
Ar	Archimedes number
c	unit cost
D	pipeline internal diameter
e	exponent in Darby (2001) model
E	energy consumption (Eq. (3))
f	Darcy friction factor
Fr	Froude number
k	design constant for minimum velocity
K	energy dissipation constant
$\dot{m}$	dry solids flow
p	pressure
Q	flow rate
Re	Reynolds number
P	dimensionless number (Eq. (15))
S	specific gravity of solids
T	time per period
u	horizontal component of velocity
W	water consumption (volume/period)

Greek letters

α	prefactor
β	exponent
γ	constant
$\in$	efficiency of pumping system
λ	pipeline utilization fraction
μ	liquid dynamic viscosity
η	Bingham plastic viscosity
ϕ	solids volume fraction
Π	dimensionless number (Eq. (16))
Ψ	dimensionless number (Eqs. (17b) and (20b))
ρ	density
τ	shear stress
$\widehat{\tau}$	yield stress prefactor (Eq. (8))
Ω	cost function

Subscripts

0	general definition
50	median size
*	transitional regime value
c	critical condition
d	deposit condition
E	related to energy
l	liquid
lam	laminar flow
m	slurry (solid–liquid mixture)
min	minimum condition
p	pumping system
ss	loose packing (settled solids) condition
t	laminar-turbulent transition condition
turb	turbulent flow
W	related to water
y	yield (applied to the concept of yield stress)

References

ANEEL, 2013. Average electric fares per region. Visited 23rd october 2013. In portugese. URL http://www.aneel.gov.br/.
Asad, M., 1999. Management of Water Resources: Bulk Water Pricing in Brazil. World Bank.
Barnes, H.A., 2000. A Handbook of Elementary Rheology. University of Wales, Institute of Non-Newtonian Fluid Mechanics Aberystyth, England.
Betinol, R.G., Jaime, H.E., 2004. Startup of dual concentrate pipeline for Minera Escondida Limitada, Phase IV. In: 16th International Conference on Hydrotransport, Santiago, Chile.
Chhabra, R.P., Richardson, J.F., 2008. Non-Newtonian Flow and Applied Rheology. Butterworth-Heinemann, Oxford, England.
Chilton, R.A., Stainsby, R., 1998. Pressure loss equations for laminar and turbulent non-Newtonian pipe flow. J. Hydraul. Eng. 124, 522, 1929.
Correa, R., Chapman, J.P., Miler, A., Alves, T., 2011. Start-up of the second SAMARCO iron concentrate pipeline. In: Proceedings of the Rio Pipeline Conference, Rio de Janeiro, Brazil.
Darby, R., 2001. Chemical Engineering Fluid Mechanics. CRC.
Del Campo, S., 2012. Estrategia Nacional de Energía 2012–2030. In. Ministerio de Energía, Gobierno de Chile, Spanish. URL http://www.minenergia.cl/estrategia-nacional-de-energia-2012.html.
Heymann, L., Peukert, S., Aksel, N., 2002. On the solid-liquid transition of concentrated suspensions in transient shear flow. Rheol. Acta 41 (4), 307–315.
Hilson, G., 2003. Defining "cleaner production" and "pollution prevention" in the mining context. Miner. Eng. 16 (4), 305–321.
Hilson, G., Nayee, V., 2002. Environmental management system implementation in the mining industry: a key to achieving cleaner production. Int. J. Miner. Process. 64 (1), 19–41.
Ihle, C.F., 2013. A cost perspective for long distance ore pipeline water and energy utilization. Part I: optimal base values. Int. J. Miner. Process. 122, 1–12.
Ihle, C.F., 2014. The need to extend the study of greenhouse impacts of mining and mineral processing to hydraulic streams: long distance pipelines count. J. Cleaner Prod. 84, 597. http://dx.doi.org/10.1016/j.jclepro.2012.11.013.
Ihle, C.F., Montserrat, S., Tamburrino, A., 2013. A cost perspective for long distance ore pipeline water and energy utilization. Part II: effect of input parameter variability. Int. J. Miner. Process. 122, 54–58.
Ihle, C.F., Tamburrino, A., 2012a. A note on the Buckingham equation. Can. J. Chem. Eng. 90, 944–945.
Ihle, C.F., Tamburrino, A., 2012b. Uncertainties in key transport variables in homogeneous slurry flows in pipelines. Miner. Eng 32, 54–59.
Ihle, C.F., Tamburrino, A., 2012c. Variables affecting energy efficiency in turbulent ore concentrate pipeline transport. Miner. Eng. 39, 62–70.
Jacobs, B., 1991. Design of Slurry Transport Systems. Elsevier, London, England.
Jenkins, H., 2004. Corporate social responsibility and the mining industry: conflicts and constructs. Corporate Soc. Respons. Environ. Manage. 11 (1), 23–34.
Jenkins, H., Yakovleva, N., 2006. Corporate social responsibility in the mining industry: exploring trends in social and environmental disclosure. J. Clean. Prod. 14 (3), 271–284.
McKinney, M.J., 1988. Water resources planning: a collaborative, consensus-building approach. Soc. Nat. Resour. 1 (1), 335–349.
Murguía, D.I., Böhling, K., 2013. Sustainability reporting on large-scale mining conflicts: the case of Bajo de la Alumbrera, Argentina. J. Clean. Prod. 41, 202–209.

Newbold, J., 2006. Chile's environmental momentum: ISO 14001 and the large-scale mining industry–case studies from the state and private sector. J. Clean. Prod. 14 (3), 248–261.
Norgate, T., Haque, N., 2010. Energy and greenhouse gas impacts of mining and mineral processing operations. J. Clean. Prod. 18 (3), 266–274.
Nouar, C., Frigaard, I., 2001. Nonlinear stability of Poiseuille flow of a Bingham fluid: theoretical results and comparison with phenomenological criteria. J. Non-Newtonian Fluid Mech. 100 (1), 127–149.
Oyarzún, J., Oyarzún, R., 2011. Sustainable development threats, inter-sector conflicts and environmental policy requirements in the arid, mining rich, northern Chile territory. Sust. Develop. 19 (4), 263–274.
Poloski, A.P., Etchells, A.W., Chun, J., Adkins, H.E., Casella, A.M., Minette, M.J., Yokuda, S.T., 2010. A pipeline transport correlation for slurries with small but dense particles. Can. J. Chem. Eng. 88, 182–189.
Roth, I.F., Ambs, L.L., 2004. Incorporating externalities into a full cost approach to electric power generation life-cycle costing. Energy 29 (12), 2125–2144.
Shook, C.A., Gillies, R.G., Sanders, R.S.S., 2002. Pipeline Hydrotransport: With Applications in the Oil Sand Industry. Saskatchewan Research Council Pipe Flow Technology Centre.
Silva, A.M., Passos, A.C., Santos, D., Orban, E.M., Lisboa, H.D., Gonçalves, N., Guimarães, R.C., 2009. Overview of the long distance iron ore slurry pipeline from Anglo Ferrous Brazil. In: Proceedings of the Rio Pipeline Conference, Rio de Janeiro, Brazil.
Slatter, P., Wasp, E.J., September 2000. The laminar/turbulent transition in large pipes. In: 10th International Conference on Transport and Sedimentation of Solid Particles — Wroclaw, pp. 389–399.
Söderholm, P., Sundqvist, T., 2003. Pricing environmental externalities in the power sector: ethical limits and implications for social choice. Ecol. Econ. 46 (3), 333–350.
Sofofa, September 2013. Precio promedio de la energía para grandes mineras llega a su menor nivel desde 2007. Visited 23rd October 2013. In Spanish. URL http://web.sofofa.cl/.
Thomas, A.D., Wilson, K.C., 1987. New analysis of non-Newtonian turbulent flow and yield-power-law fluids. Can. J. Chem. Eng. 65 (2), 335–338.
Viscusi, K., Magat, W., Carlin, A., Dreyfus, M., 1994. Environmentally responsible energy pricing. Energy J. 15 (2).
Wilson, K.C., Thomas, A.D., 1985. A new analysis of the turbulent flow of non-Newtonian fluids. Can. J. Chem. Eng. 63 (4), 539–546.
Wu, J., Graham, L., Wang, S., Parthasarathy, R., 2010. Energy efficient slurry holding and transport. Miner. Eng. 23 (9), 705–712.